High-throughput phenotypic profiling for bioactivity screening of environmental chemicals

Johanna Nyffeler[1,2], Clinton Willis[1,3], Katie Paul Friedman[1], Imran Shah[1], John Wambaugh[1], Joshua Harrill[1]

[1] Center for Computational Toxicology and Exposure, Office of Research and Development, US Environmental Protection Agency, Durham, NC 27711, United States.
[2] Oak Ridge Institute for Science and Education (ORISE) Postdoctoral Fellow, Oak Ridge, TN, 37831, United States. [3] Oak Ridge Associated Universities (ORAU) National Student Services Contractor, Oak Ridge, TN,

Johanna Nyffeler | Nyffeler.Johanna@epa.gov | 000-000-0000

www.epa.gov

Background

- Image-based phenotypic profiling is a chemical screening method that measures a large variety of morphological features of individual cells in *in vitro* cultures.
- Successfully used for functional genomic studies and in the pharmaceutical industry for compound efficacy and toxicity screening.
- No requirement for *a priori* knowledge of molecular targets.

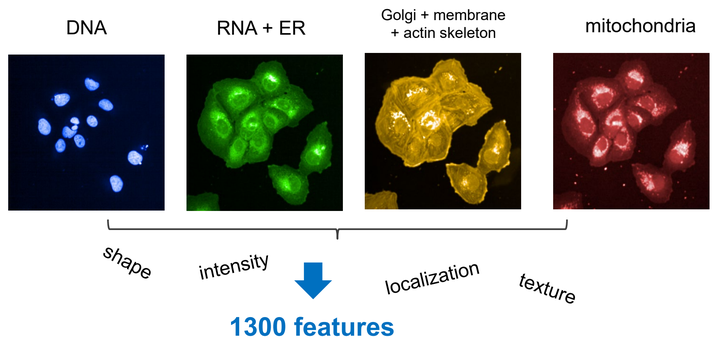

⇨ **May be used as an efficient and cost-effective method for evaluating the bioactivity of environmental chemicals.**

⇨ **May be used to determine bioactivity thresholds (i.e. *in vitro* point-of-departure, POD) for comparison to effect values from animal studies (i.e. *in vivo* POD) and predicted exposure levels.**

⇨ **May potentially be used to identify putative mechanism(s)-of-action of environmental chemicals.**

Aims

1. **Adapt an existing assay (Bray et al. 2016) to be compatible with EPA liquid handling and imaging instruments & develop analysis pipelines for high-throughput concentration-response screening.**
2. **Identify reference chemicals to monitor assay performance.**
3. **Screen a set of 462 environmental chemicals and derive *in vitro* points-of-departure (PODs).**
4. **Compare the PODs to other new approach methodologies (NAMs), to *in vivo* effect values and to predicted exposure levels.**
5. **Investigate whether profiles can provide information on mechanisms-of-action.**

Phenotypes & reproducibility of reference chemicals

A set of 14 chemicals with specific phenotypes in a previous study (Gustafsdottir et al. 2013) were tested. Four chemicals with large phenotypic effects were chosen as reference chemicals:

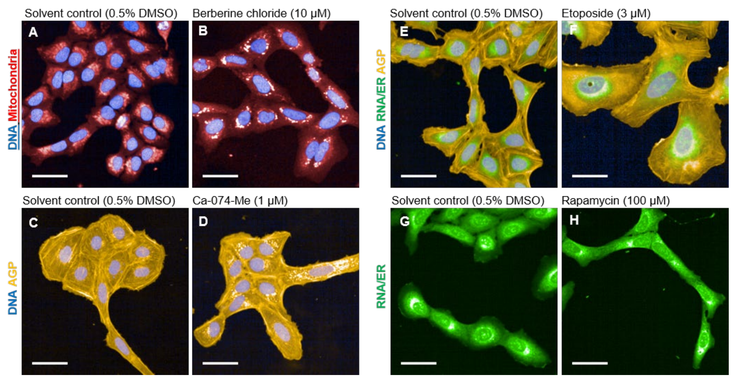

Fig. 3: Examples of chemical-specific cytological phenotypes. U-2 OS cells were treated for 48 h with the compounds before cells were live-labeled for mitochondria, fixed, permeabilized and remaining labels applied. Images were acquired with a 20x water immersion objective. Only selected channels are shown to highlight the phenotypes.

⇨ **Phenotypes are mostly consistent with literature (Gustafsdottir *et al.* 2013)**

⇨ **Different chemicals induce different cytological phenotypes**

The four reference chemicals were run on each plate of the screen to evaluate reproducibility of profiles and of PODs:

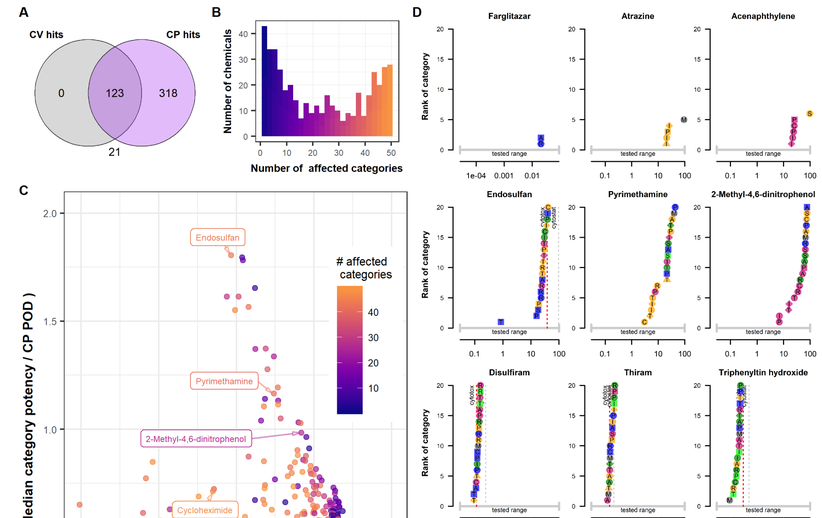

Fig. 4: Evaluation of CP assay performance. (A) Well-level feature data was normalized and scaled per plate and then averaged within plate group. The columns of the heatmap correspond to the 1300 features, organized by fluorescent channel. Tile colors represent the magnitude of increase or decrease in a measured feature with respect to DMSO control. Each row represents data from a plate group. One concentration per chemical that produced marked phenotypic effects is shown: Berberine chloride (10 µM), Ca-074-Me (0.3 µM), Etoposide (0.3 µM), Rapamycin (3 µM). (B) Correlation of CP profiles. Data was normalized and scaled per plate and then averaged within plate group. Normalized area under the curve (nAUC) was computed for each endpoint. The nAUC is defined as the summed effect sizes across all non-cytotoxic doses. Each row/column represents data from a plate group and the profiles were compared to each other using Spearman correlation coefficient.(C) Reproducibility of CP PODs. Well-level data was used for concentration-response modeling with BMDExpress. The CP POD is defined as the median concentration of the most sensitive category that had ≥ 30% affected endpoints. The vertical dotted line indicates the lowest tested concentration. If the POD was below the tested range, the POD was set as half an order of magnitude below the lowest tested concentration.

⇨ **profiles are reproducible across different plates**

⇨ **POD varies by less than 1 order of magnitude across plates**

Screening results

Fig. 5: HTPP screening summary. (A) Comparison of hits for the CV and CP assays. A total of 462 unique chemicals were screened. (B) Histogram of the number of affected categories across all positive chemicals (n = 441). (C) Scatterplot of the CP POD (log10, µM) versus the ratio of the median category potency to the CP POD (defined as the most sensitive category potency). Each point represents a chemical that was positive in the HTPP assay. (D) Accumulation plots for exemplary chemicals labeled in panel C. The feature-level BMCs were grouped into 49 categories. Categories where ≥ 30% of the constituent features were concentration-responsive were ranked in ascending order according to the median BMC of the category. Only the 20 most potent categories are shown. The onset of cytotoxicity and cytostatic effects are marked by red and gray vertical dotted lines, respectively. Absence of vertical lines indicates that cytotoxicity or cytostatic effects were not observed within the concentration range tested.

⇨ **95% of compounds were identified as bioactive with the profiling assay**

⇨ **some affected only few features/categories, others have broad effects**

⇨ **affected categories vary among chemicals**

Conclusions

1. **Published results could be reproduced; distinct phenotypic profiles were observed.**
2. **Reference chemicals produced reproducible profiles and their PODs varied by less than 1 order of magnitude among plates.**
3. **95% of chemicals screened were bioactive; a variety of profiles were observed.**
4. **The HTPP PODs correlated well with *in vivo* PODs and were less conservative than other alternative approaches. For the majority of chemicals the predicted exposure was > 1000x lower than bioactivity.**
5. **Chemicals with similar cellular effects have similar profiles. Structural similar chemicals may produce similar profiles.**

Comparison to other NAMs and *in vivo* toxicity

HTPP PODs were converted to administered equivalent doses and compared to *in vivo* effect values and published NAM results:

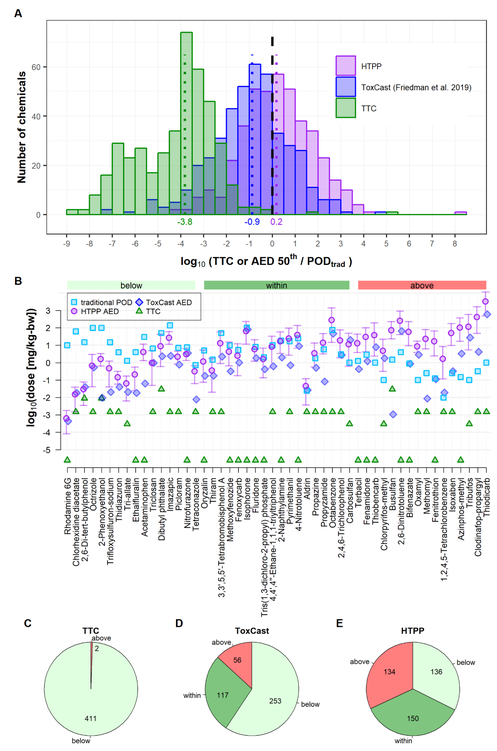

Fig. 6: Comparison of HTPP assay results to *in vivo* toxicity values and published NAM results. (A) Comparison of different NAMs to the *in vivo* POD (POD_{trad}). HTPP PODs were used to calculate an administered equivalent dose (HTPP AED) that would correspond to a plasma concentration equivalent to the HTPP POD in a human population. Vertical dotted lines and numbers below indicate the median of the distribution for each NAM. The vertical dashed line indicates the unity line. The histogram comprises only chemicals that had available *httk* and *in vivo* data (ToxCast n=426, TTC n=413, HTPP n=420 (only HTPP hits)). (B) IVIVE results for representative chemicals. Chemicals were sorted according to the difference between the HTPP AED distribution and the *in vivo* POD.(C) Chemicals in the "above" group had AEDs that overpredicted the *in vivo* effect dose. Chemicals in the two latter groups provided either a comparable (POD_{trad} lies within the AED range) or conservative surrogate for the *in vivo* effect dose, respectively. As for the TTC approach no dose range exists, the chemicals were grouped into "above" and "below" only.

⇨ **HTPP AEDs are less conservative than ToxCast-derived AEDs and TTC values**

⇨ **81% of HTPP AED are within 2 orders of magnitude of the *in vivo* POD**

Comparison to exposure estimates

HTPP AEDs were compared to exposure predictions and the bioactivity-exposure ratio was calculated as follows:

$$\text{BER} = \frac{\text{lower bound of HTPP bioactivity}}{\text{upper bound of exposure estimate}} = \log_{10}\left(\frac{\text{HTPP AED } 5^{\text{th}}}{\text{SEEM3 } 95^{\text{th}}}\right)$$

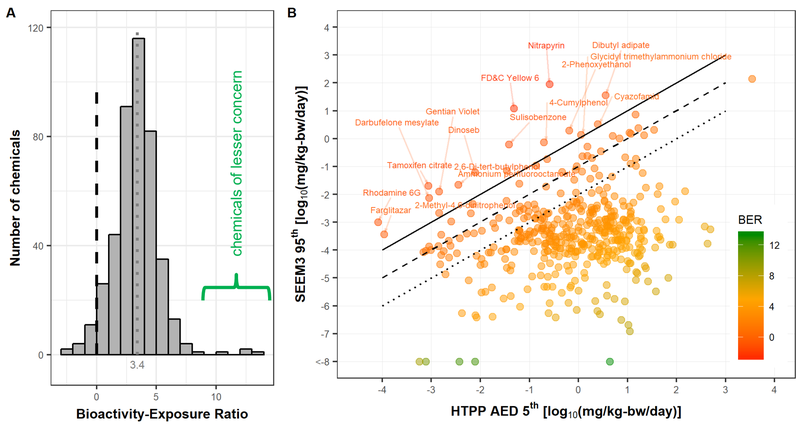

Fig. 7: Comparison of HTPP assay results to exposure predictions. (A) The bioactivity-exposure ratio (BER) was defined as the ratio of the lower bound of the HTPP AED confidence interval and the upper bound of the exposure prediction from the SEEM3 framework. The gray dotted line indicates the median of the distribution. For chemicals to the left of the unity line (vertical dashed line), the bioactivity and exposure estimates overlap, indicating a potential for humans to be exposed to bioactive concentrations of these chemicals. (B) The 17 chemicals with a negative BER are labeled (n = 433 chemicals).

⇨ **for 59% of chemicals, predicted exposure is > 1000x lower than estimated bioactivity**

⇨ **for 3.9% (17/433) of chemicals, the BER was negative, indicating a potential for humans to be exposed to bioactive concentrations of these chemicals**

Profile comparison

Phenotypic profiles of chemicals can be compared to identify chemicals with similar cellular effects:

Example 1: Various types of DNA toxicants result in similar profiles

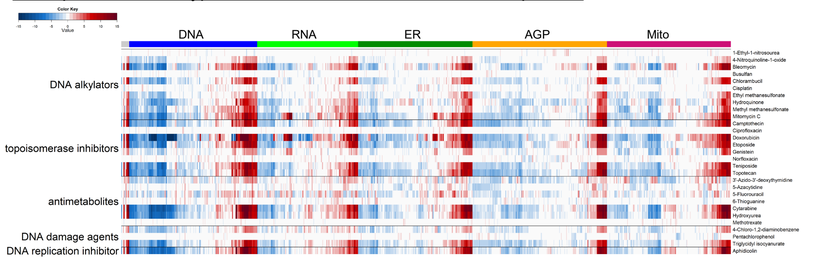

Fig. 8: Comparison of profiles. For each chemical, a profile was generated by taking for each feature the largest effect size observed at non-cytotoxic concentrations (= magnitude). Then, a signature was derived by flooring all |values| < 1.5 to 0. Mechanisms-of-action derived from literature are indicated on the left.

⇨ **Chemicals with similar cellular effects produce similar profiles**

Example 2: Organochlorines share a characteristic profile

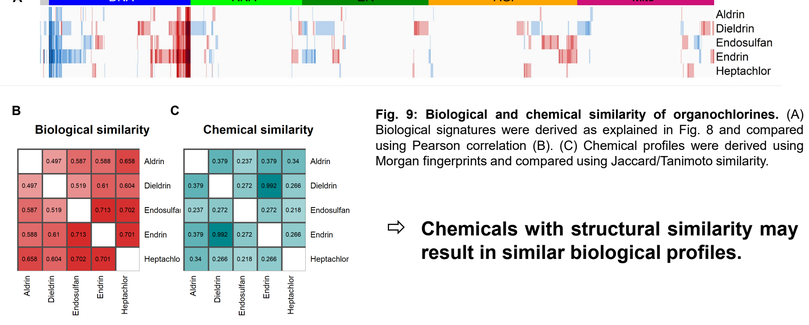

Fig. 9: Biological and chemical similarity of organochlorines. (A) Biological signatures were derived as explained in Fig. 8 and compared using Pearson correlation (B). (C) Chemical profiles were derived using Morgan fingerprints and compared using Jaccard/Tanimoto similarity.

⇨ **Chemicals with structural similarity may result in similar biological profiles.**

Methods

1. Experimental workflow

Experiments were conducted in 384 well format using microfluidics tools and a high content screening microscope:

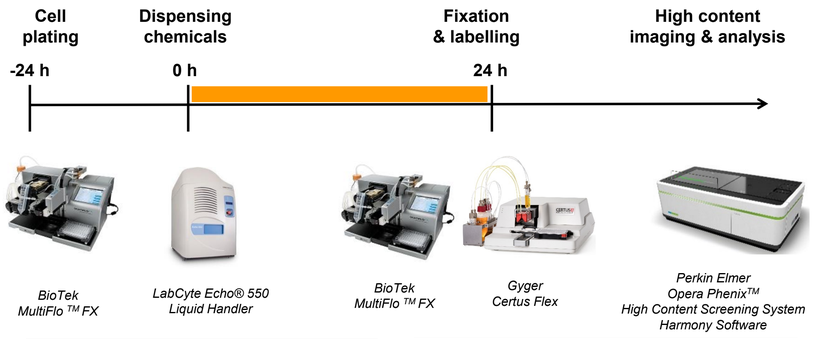

Experimental design	
Cell type	U-2 OS
Exposure time	24 h
# chemicals	462
# concentrations	8
Concentration spacing	½ $\log_{10}$
Solvent controls/plate	24
Replicates/plate	1
# independent experiments	4
Reference chemicals (per plate)	5 chemicals 6 concentrations

Cell Profiling (CP)	
Organelle/Structure	**Label**
DNA	H-33342
RNA	SYTO14
ER	Concanavalin A-488
Actin	Phalloidin-568
Golgi + Membrane	wheat germ agglutinin (WGA) -555
Mitochondria	MitoTracker

Cell Viability (CV)	
Structure	**Label**
DNA	H-33342
Dying cells	Propidium iodide (PI)

2. Image & data analysis

For each set of chemicals, two assays were run in parallel:

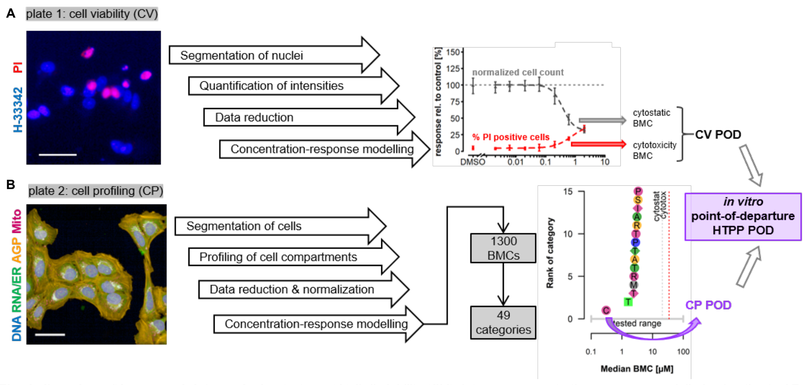

Fig. 1: Overview of image and data analysis strategy. (A) Cell viability (CV) data was concentration-response modelled using the *tcpl* R package. Benchmark concentrations (BMC) were derived for two endpoints: for cytostatic effects (reduction in cell number) and cytotoxicity (increase in the proportion of dying cells). The minimum of the two was defined as the CV point-of-departure (CV POD) (B) Cell profiling (CP) data was clipped above the CV POD before concentration-response modelling with BMDExpress 2.2. The benchmark concentrations (BMCs) of the 1300 features were then grouped into 49 categories. A category was considered affected if ≥ 30% of the features were affected (i.e. had a BMC). The median BMC of the most sensitive category was defined as the CP POD. The minimum of CV POD and CP POD was defined as the HTPP POD.

3. Comparison to other bioactivity measures and exposure

In vitro-to-*in vivo* extrapolation (IVIVE) was performed using reverse dosimetry to extrapolate the HTPP POD to an administered equivalent dose (AED) to compare it with *in vivo* effect values, other alternative methods and to exposure predictions:

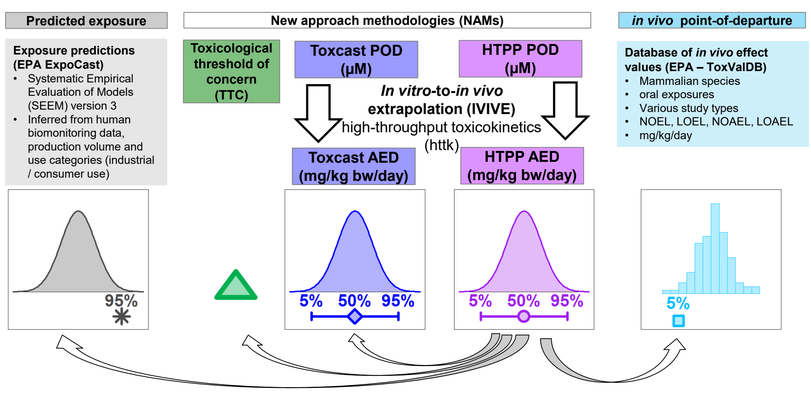

Fig. 2: Procedure to compare *in vitro* POD (in µM) to *in vivo* bioactivity data (in mg/kg bw/day), other alternative approaches and exposure. Administered equivalent doses (AEDs) that would give a plasma concentration corresponding to the *in vitro* POD were estimated using high-throughput toxicokinetic information and models in the *httk* R package (v1.8). The displayed interval indicates inter-individual variability in toxicokinetics (5-95%). The AED was then compared to *in vivo* data from the ToxValDB database. In this study, the *in vivo* POD was defined as the 5th percentile of the distribution of available effect values. Additionally, the HTPP AED was compared to two other alternative methods: A POD from a collection of Toxcast assays was calculated in a previous study (Paul-Friedman et al. 2019). The same study also reported toxicological thresholds of concern (TTC) values. The upper confidence bound of exposure was predicted using SEEM3 model (Wambaugh, et al. 2014).

4. Profile comparison

1. Profile generation

   Effect sizes were summarized across concentrations by retaining the largest effect size (= magnitude) at non-cytotoxic concentrations for each feature

2. Signature generation

   Values for features with a |magnitude| < 1.5 were replaced with 0, to remove noise and enhance correlation of features with substantial magnitudes.

3. Comparison of signatures

   Signatures were compared using Pearson correlation. A correlation > 0.5 was considered to be indicative of similar phenotypic profiles.

References:

Bray, M. A., Singh, S., Han, H., Davis, C. T., Borgeson, B., Hartland, C., . . . Carpenter, A. E. (2016). Cell Painting, a high-content image-based assay for morphological profiling using multiplexed fluorescent dyes. *Nat Protoc, 11*(9), 1757-1774. doi:10.1038/nprot.2016.105

Gustafsdottir, S. M., Ljosa, V., Sokolnicki, K. L., Anthony Wilson, J., Walpita, D., Kemp, M. M., . . . Shamji, A. F. (2013). Multiplex cytological profiling assay to measure diverse cellular states. *PLoS One, 8*(12), e80999. doi:10.1371/journal.pone.0080999

Paul-Friedman, K., Gagne, M., Loo, L. H., Karamertzanis, P., Netzeva, T., Sobanski, T., . . . Thomas, R. S. (2019). Examining the utility of in vitro bioactivity as a conservative point of departure: a case study. *Toxicol Sci*.

Wambaugh, J. F., Wang, A., Dionisio, K. L., Frame, A., Egeghy, P., Judson, R., and Setzer, R. W. (2014). High throughput heuristics for prioritizing human exposure to environmental chemicals. *Environ Sci Technol* **48**(21), 12760-7.